2. Meyerowitz, E. M. *et al*. A genetic and molecular model for floral development in *Arabidopsis thaliana*. *Development* **1,** 157–167 (1991).
3. Irish, V. F. & Kramer, E. M. in *Advances in Botanical Research* 197–230 (Academic, San Diego, 1998).
4. Theissen, G. & Saedler, H. MADS-box genes in plant ontogeny and phylogeny Haeckel's 'biogenetic law' revisited. *Curr. Opin. Gen. Dev.* **5,** 628–639 (1995).
5. Bowman, J. L. Evolutionary conservation of angiosperm flower development at the molecular and genetic levels. *J. Biosci.* **22,** 515–527 (1997).
6. Kramer, E. M., Dorit, R. L. & Irish, V. F. Molecular evolution of genes controlling petal and stamen development: Duplication and divergence within the *APETALA3* and *PISTILLATA* MADS-box gene lineages. *Genetics* **149,** 765–783 (1998).
7. Jack, T., Brockman, L. L. & Meyerowitz, E. M. The homeotic gene APETALA3 of *Arabidopsis thaliana* encodes a MADS box and is expressed in petals and stamens. *Cell* **68,** 683–697 (1992).
8. Goto, K. & Meyerowitz, E. M. Function and regulation of the *Arabidopsis* floral homeotic gene PISTILLATA. *Genes Dev.* **8,** 1548–1560 (1994).
9. Purugganan, M. D., Rounsley, S. D., Schmidt, R. J. & Yanofsky, M. F. Molecular evolution of flower development: Diversification of the plant MADS-box regulatory gene family. *Genetics* **140,** 345–356 (1995).
10. Bowman, J. L., Smyth, D. R. & Meyerowitz, E. M. Genes directing flower development in *Arabidopsis*. *Plant Cell* **1,** 37–52 (1989).
11. Zachgo, S. *et al*. Functional analysis of the *Antirrhinum* floral homeotic *Deficiens* gene *in vivo* and *in vitro* by using a temperature-sensitive mutant. *Development* **121,** 2861–2875 (1995).
12. Sommer, H. *et al*. Properties of *deficiens*, a homeotic gene involved in the control of flower morphogenesis in *Antirrhinum majus*. *Development* **1** (suppl.), 169–175 (1991).
13. Ronse Decraene, L. P. & Smets, E. F. An updated interpretation of the androecium of the Fumariaceae. *Can. J. Bot.* **70,** 1765–1776 (1992).
14. Kelly, A. J., Bonnlander, M. B. & Meeks-Wagner, D. R. NFL, the tobacco homolog of floricaula and leafy, is transcriptionally expressed in both vegetative and floral meristems. *Plant Cell* **7,** 225–234 (1995).
15. Hardenack, S., Ye, D., Saedler, H. & Grant, S. Comparison of MADS box gene expression in developing male and female flowers of the dioecious plant white campion. *Plant Cell* **6,** 1775–1787 (1994).
16. Takhtajan, A. *Evolutionary Trends in Flowering Plants* (Columbia Univ. Press, New York, 1991).
17. Drinnan, A. N., Crane, P. R. & Hoot, S. B. in *Early Evolution of Flowers* (eds Endress, P. K. & Friis, E. M.) 93–122 (Springer, New York, 1994).
18. Kosuge, K. Petal evolution in Ranunculaceae. *Plant Syst. Evol.* **8** (suppl.), 185–191 (1994).
19. Carr, S. & Irish, V. Floral homeotic gene expression defines developmental arrest stages in *Brassica oleracea* L. vars. *botrytis* and *italica*. *Planta* **201,** 179–188 (1997).
20. Lincoln, C., Long, J., Yamaguchi, J., Serikawa, K. & Hake, S. A knotted1-like homeobox gene in *Arabidopsis* is expressed in the vegetative meristem and dramatically alters leaf morphology when overexpressed in transgenic plants. *Plant Cell* **6,** 1859–1876 (1994).
21. Smith, L., Greene, B., Veit, B. & Hake, S. A dominant mutation in the maize homeobox gene, *Knotted-1*, causes its ectopic expression in leaf cells with altered fates. *Development* **116,** 21–30 (1992).
22. Chase, M. W. *et al*. Phylogenetics of seed plants: an analysis of nucleotide sequences from the plastid gene rbcL. *Ann. Missouri Bot. Gard.* **80,** 528–580 (1993).

Acknowledgements. We thank P. Jenik for antibody preparation, and I. Dawson, P. Jenik, T. Hill, C. Juarez, R. Lamb and Q. Tan for comments on the manuscript. This work was supported by grants from the NSF and USDA to V.F.I.

Correspondence and requests for materials should be addressed to V.F.I. (e-mail: vivian.irish@yale.edu).

The role of the anterior prefrontal cortex in human cognition

Etienne Koechlin, Gianpaolo Basso, Pietro Pietrini, Seth Panzer & Jordan Grafman

Cognitive Neuroscience Section, National Institute of Neurological Disorders and Stroke, National Institutes of Health, Bethesda, Maryland 20892-1440, USA

Complex problem-solving and planning involve the most anterior part of the frontal lobes including the fronto-polar prefrontal cortex (FPPC)[1–6], which is especially well developed in humans compared with other primates[7,8]. The specific role of this region in human cognition, however, is poorly understood. Here we show, using functional magnetic resonance imaging, that bilateral regions in the FPPC alone are selectively activated when subjects have to keep in mind a main goal while performing concurrent (sub)goals. Neither keeping in mind a goal over time (working memory) nor successively allocating attentional resources between alternative goals (dual-task performance) could by themselves activate these regions. Our results indicate that the FPPC selectively mediates the human ability to hold in mind goals while exploring and processing secondary goals, a process generally required in planning and reasoning.

This process of integrating working memory with attentional resource allocation is referred to as branching. In everyday life, branching is frequently required: for example, if a person is interrupted with a question while reading. As in dual-task performance, branching successively allocates processing resources between concurrent tasks (such as listening and reading). As in delayed-response performance, branching keeps relevant information in working memory to allow a return to the main task after completing a secondary task (in our example, remembering and returning to where you left off reading). Knowing that problem-solving and planning involve the FPPC[1–6] and generally involve branching, whenever goal-tree sequences are processed we proposed that only fronto-polar regions would be selectively engaged by the integration of working memory and attentional-resource allocation.

Table 1 Factorial design of the experiment

Attentional resource allocation	Working memory	
	No delayed response	Delayed response
Single-task performance	Control	Delay
Dual-task performance	Dual task	Branching

Using functional magnetic resonance imaging (fMRI), we employed a 2×2 factorial design crossing delayed-response and dual-task performance (Table 1), so that subjects performed an on-line letter-matching task in four conditions including a control, a delay, a dual-task and a branching condition (see Figs 1 and 2). Accordingly, specific branching activations were specified as an interaction between delayed-response and dual-task performance and were expected to be found only in fronto-polar regions.

The fMRI results confirm our prediction (Table 2 and Figs 3–5). First, we tested for regions selectively involved in either dual- or delayed-task performance (see Methods). The main effect of dual-task performance was found to involve, selectively and bilaterally, the posterior dorsolateral prefrontal cortex (BA (Brodman's area) 9, middle frontal gyrus, close to the pre-central gyrus and BA 8) and the lateral parietal cortex (inferior parietal lobule, BA 40). In accordance with previous studies, this confirms that this network of brain areas is involved in allocating attentional resources between successively alternating tasks or stimuli[9,10]. In contrast, the main effect of delayed performance involved no specific brain region even

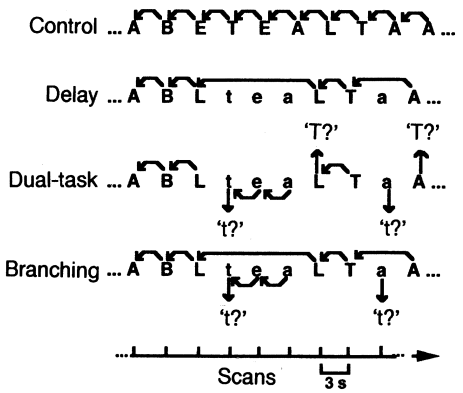

Figure 1 Behavioural tasks. Stimuli were pseudorandom sequences of upper- or lower-case letters from the word 'tablet'. Control condition: subjects had to decide whether two successively presented letters were also in immediate succession in the word 'tablet' (only upper-case letters were presented). Delay condition: subjects had to ignore lower-case letters which were used to occasionally delay the response required by the control condition. Dual task condition: subjects had to respond as in the control condition for both upper- and lower-case letter series with one exception. Subjects had to decide whether every first letter indicating a case change was the letter T (or t). Branching condition: subjects had to respond to upper-case letters exactly as in the delay condition and to lower-case letters exactly as in the dual-task condition.

Table 2 Coordinates and *Z*-score for maxima of activations

Regions Brodman's area*	Talairach coordinates†	Statistical effects (*Z*-value)‡						
		BR-CR	DE-CT	DT-CT	BR-DE	BR-DT	DE-DT	DT-DE
Interaction								
Right, BA 10, GFp	36, 66, 21	8.2	n.s.	n.s.	6.8	6.8	n.s.	n.s.
Left, BA 10, GFp	–36, 57, 9	8.1	n.s.	n.s.	6.2	7.3	n.s.	n.s.
Additivity								
Right, BA 10, GFs	30, 75, 12	8.5	6.8	7.6	7.0	5.2	n.s.	n.s.
Right, BA9/46, GFm	54, 36, 30	8.5	6.5	7.9	7.1	3.9	n.s.	n.s.§
Right BA 7, Pcu	6, –60, 48	8.3	6.1	7.5	6.1	3.6	n.s.	n.s.
Main effects (dual task)								
Right, BA 9/8, GFm	45, 21, 36	8.3	5.3	8.1	6.8	n.s.	n.s.	5.6
Right, BA 40, LPi	48, –39, 48	7.7	n.s.	8.0	6.5	n.s.	n.s.	7.3
Left, BA 9/8, GFm	–45, 27, 36	7.9	n.s.	7.3	7.2	n.s.	n.s.	5.6
Left, BA 7, LPs	–42, –51, 54	8.3	n.s.§	8.2	7.7	n.s.	n.s.	7.3

Data relate to maxima of activations shown in Fig. 3.
* BA, Brodman's area; GF, frontal gyrus; LP, parietal lobule; i, inferior; m, middle; s, superior; p, polar; Pcu, precuneus.
† Talairach coordinates of maxima in contrast branching minus control conditions.
‡ BR, branching; DE, delay; DT, dual-task; CT, control. n.s. not significant ($P > 0.9$, corrected).
§ $P > 0.5$, corrected.

at low statistical thresholds. This indicates that the duration of delay during which information is maintained on-line in this task is not in itself a main factor triggering the activation of specific cortical regions.

Our main aim was to identify brain regions involved in both delayed-response and dual-task performance. Those regions fall into one of two categories: regions that exhibit additive effects, where the evoked response is simply explained by the activation due to utilizing working memory or attention allocation independently; and regions that show an interaction, where there is a super-additive component that is attributable to the cognitive integration of working memory and attentional allocation (in our framework, a branching process).

Additive activations were obtained by selecting the regions engaged in all experimental conditions compared with baseline (see Methods). No interaction was observed *post hoc* in those regions ($P > 0.05$), namely the right anterior dorsolateral prefrontal cortex (BA 9/46, middle frontal gyrus), the right superior frontal gyrus (BA 10) and the right precuneus (BA 7) (Figs 3 and 5). When compared to the control condition, the MR signal change recorded in these brain regions during the branching condition co-varied with the sum of the signal changes in the delay and dual-task conditions. This cortical network is involved in episodic memory tasks, becoming activated when the circumstances in which events occurred are retrieved[11–16]. In accordance with these results, all but the control conditions in our experiment share the common feature that subject performance depends upon processing and retrieving the context in which a stimulus occurs (either its lower/upper case status on a given trial or the task rules on a given experimental block). Performance in the branching condition required subjects to combine the previously independent contextual information used in the delay and dual-task conditions, which may explain the additivity effect found in these regions.

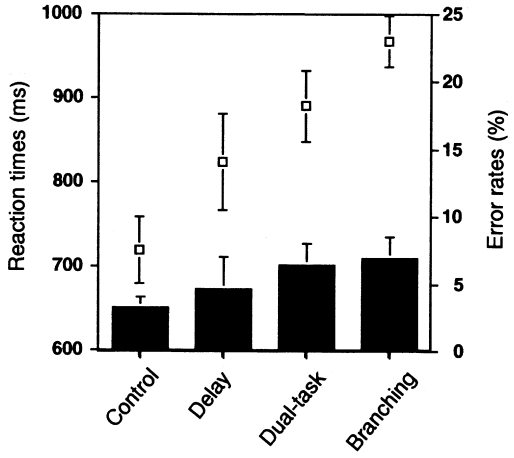

Figure 2 Behavioural performance. Symbols: increases in reaction times (mean ± s.e. in ms) across conditions ($F(3, 15) = 14.6$, $P < 0.0001$), confirming that additional processes and regions are engaged successively in the control, delay, dual-task and branching conditions. Bars: error rates (mean ± s.e. in percentage) remained very similar across conditions ($F(3, 15) = 1.2$, $P > 0.34$) with virtually no difference between the dual-task and branching conditions.

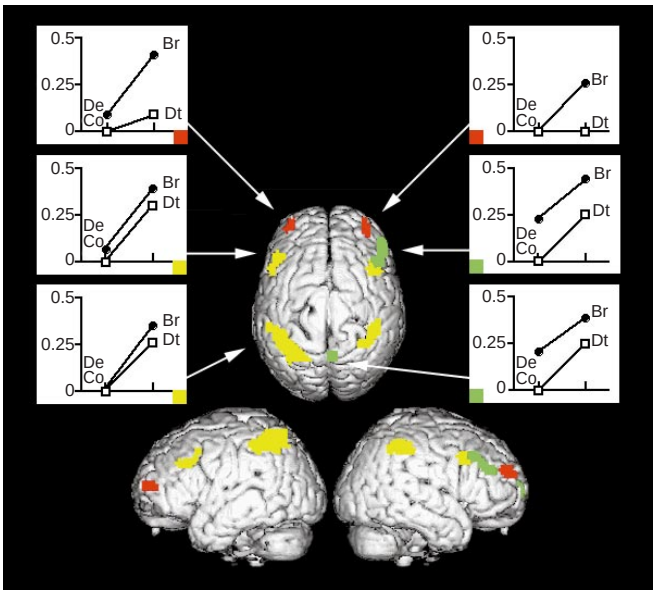

Figure 3 Topography of brain regions with distinct activation profiles. Yellow, main effects of dual-task performance. Green, additivity of the dual-task and delayed-response performance effects. Red, Interaction of dual-task and delayed-performance effects or branching-specific activations. See Methods for details and Table 2 for coordinates of activation foci. Inserts, data points are the mean signal changes (vertical axis, percentage) in the delay (De), dual-task (Dt) and branching (Br) conditions (measured in the stationary state, that is, in the second half-block) relative to the adjusted signal mean in the control condition (Co).

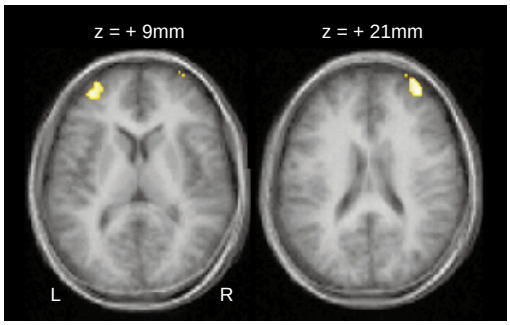

Figure 4 Branching-specific activations (*Z*-maps thresholded at $Z > 4.5, P < 0.05$, corrected) superimposed on anatomical axial slices averaged across subjects (Talairach coordinates $Z = 9$ and 21 mm). See Fig. 3 for details.

Super-additive, or branching-specific, activation was obtained by selecting regions which were engaged in the branching condition compared with baseline and, in addition, showed a significant interaction between working memory and attentional allocation factors (see Methods). As predicted, this revealed only two regions, located symmetrically in the left and right dorsal FPPC (BA 10, fronto-polar gyrus; Figs 3 and 4). In both regions, the MR signal increased significantly in the branching condition, but was quantitatively similar in all other conditions (Fig. 5). As neither the delayed nor dual-task performance alone significantly activated these regions, these results indicate that these fronto-polar regions are crucial only when branching processes are engaged. The activated foci differed slightly in the left and right fronto-polar regions, which may result from variations in the anatomy or the functional mapping between the two frontal lobes[17].

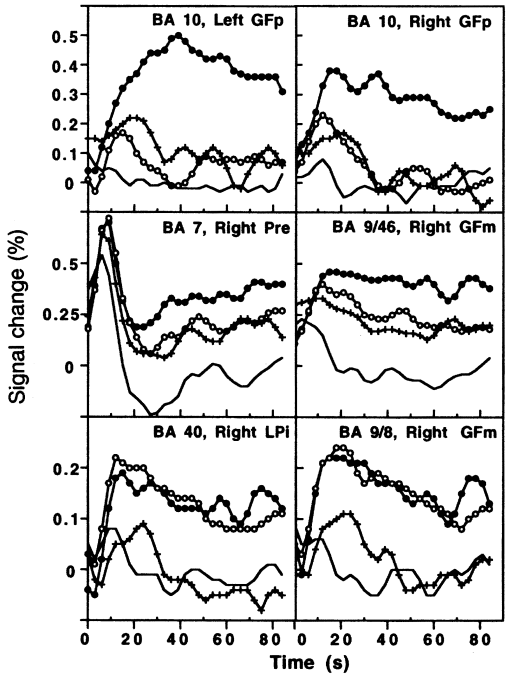

Figure 5 Dynamics of activation profiles. Plots are related to the regions shown in Fig. 3 and Table 2; *x*-axis, time measured from experimental block onsets. Stimulus onsets occur every 3 s, starting from time 3. Data points are relative signal changes averaged in every region during branching (filled circle), delay (cross), dual-task (circle) and control (no symbol) conditions. Signal changes (in per cent) are measured from the adjusted signal mean in the control condition.

Behavioural data show that these fronto-polar activations were not related to variations in mental effort alone. If that had been the case, a gradual increase in MR signal, associated with the gradual increase in difficulty of the tasks from the control to the delayed-task, dual-task and branching conditions (Fig. 2), would have been observed[18]. Instead, no difference in brain activation was found in these regions between conditions with different behavioural performances (for example, the control and dual-task conditions), whereas significant activation differences were observed between the dual-task and branching conditions despite very similar behavioural performance. Moreover, six more normal right-handed subjects (three males and three females, aged 20–28) performed the dual-task condition under more difficult constraints using degraded letters. Although subjects could still identify all letters, the task was significantly more difficult than the branching condition. Response times increased by 112 ms from the regular to the difficult dual-task condition ($P < 0.02$), and mean accuracy fell from 96.2 to 87.7%. As expected, increasing difficulty resulted in increased frontal activations in the posterior dorsolateral prefrontal cortex and the anterior cingulate cortex, but not in the FPPC ($Z < 1.0$, $P > 0.15$) in contrast to the results predicted by a mental effort interpretation of our data.

In summary, distinct dorsal fronto-polar regions were selectively engaged in branching processes when compared with other executive processes including working memory[19–22], attentional resource allocation[9,10] and processing episodic information[11–16]. This finding may clarify why the FPPC was found to be engaged in complex problem-solving[1–6] and, incidentally, in working-memory tasks performed in dual-task contexts[2,3,23,24]. These branching-specific regions may have a key role in processing goal-tree sequences, which frequently requires the temporary interruption of a current plan to achieve subgoals, or to respond to new environmental demands or intrusive thoughts, and may help to mediate a range of human behaviours including planning and reasoning. □

Methods

Behavioural protocol. Subjects responded to visually presented letters (500 ms duration, 3,000 ms stimulus-onset-asynchrony (SOA)) by pressing response buttons with their right (match) or left (no match) hand, respectively. Matching proportions were maintained between 40 and 43% of trials in each condition. In all but the control conditions lower-case letters were pseudorandomly presented in 64% of trials and the mean SOA between two successive upper-case letters was strictly maintained at 6.3 s. In the delay condition, subjects were asked to ignore lower-case letters by always pressing the no-match button (see Fig. 1 legend for details). The task was administered in six scanning runs using the Expe software package[25]. Each condition was included once in each run as a block of 28 trials. The resulting 24 blocks were pseudorandomly ordered so that each condition appears at all serial positions within a run and two conditions appeared once or twice in immediate succession to prevent confounding order effects. Subjects were given standard instructions to respond quickly and accurately. Behavioural and fMRI data were recorded simultaneously from six right-handed subjects (three females and three males, aged 20–28 years) who were trained and reached a threshold accuracy (>70%) in all conditions before and during scanning. Three additional subjects were excluded because they did not reach this threshold during scanning. Subjects provided written informed consent approved by the NIH.

Image acquisition and analysis. A standard 1.5 GE signa scanner whole-body and RF coil scanner were used to perform a high-resolution structural scan for each subject followed by six runs of 120 functional axial scans (TR 3 s, TE 40 ms, flip angle 90°; FOV 24 cm, acquisition matrix 64×64, number of slices 18, thickness 6 mm) synchronized with stimulus presentation. All fMRI data were processed using the SPM96 software package (http://www.fil.ion.ucl.ac.uk/spm/)[26] with modified memory-mapping procedures. Standard linear image realignment, linear normalization to the stereotaxic Talairach atlas (MNI template)[27], spatial (3D gaussian kernel: 10 mm) and temporal smoothing, and mean MR-signal normalization across scans were successively performed for each subject. Then, all subjects were pooled together and statistical

parametric maps (SPM) were computed from local MR signals using a linear multiple regression with conditions (modelled as two temporal basis functions) and runs as co-variates[26]. Only regions formed by more than 12 contiguious active voxels ($P < 0.05$) were analysed. The main effect of dual-task (and delayed-response, respectively) performance was computed by selecting the regions which were co-jointly significantly activated in the dual-task (delay) and branching conditions compared with the control and delay (dual-task) conditions ($Z > 5.4$, $P < 0.0005$, corrected for multiple comparisons). The additive effect of delay and dual-task performance was observed in the regions co-jointly and significantly activated in all conditions compared with the baseline ($Z > 5.4$, $P < 0.0005$, corrected). No interaction between those factors ($P > 0.05$, uncorrected) was observed in those regions. Branching-specific activations were computed as the regions with significant activations in the branching condition compared with the control ($Z > 5.4$, $P < 0.0005$, corrected) and with a significant interaction between the delayed-response and dual-task factors (branching and control compared to delay and dual-task conditions; $P < 0.0005$, uncorrected). The same branching-specific activation was found *post hoc* by computing the voxels co-jointly activated in the branching condition compared separately with all other conditions (fronto-polar: $Z > 5.4$, $P < 0.0005$, corrected; elsewhere $P > 0.05$, corrected). Branching-specific activations were confirmed in five single-subject analyses. They were located bilaterally in the superior fronto-polar gyrus at the crossing of the middle frontal gyrus (two subjects) or in the middle fronto-polar gyrus (three subjects)[28]. Moreover, bilateral fronto-polar activations were replicated in six additional normal right-handed subjects performing the branching and two additional control tasks.

Received 23 October 1998; accepted 12 March 1999.

1. Grafman, J. in *Structure and Function of the Human Prefrontal Cortex* (eds Grafman, J., Holyoak, K. J. & Boller, F.) 337–368 (Annals of the New York Academy of Sciences, New York, 1995).
2. Baker, S. C. *et al.* Neural system engaged by planning: A PET study of the Tower of London task. *Neuropsychologia* **34,** 515–526 (1996).
3. Owen, A. M., Doyon, J., Petrides, M. & Evans, A. C. Planning and spatial working memory: a positron emission tomography study in human. *Eur. J. Neurosci.* **8,** 353–564 (1996).
4. Sirigu, A. *et al.* Planning and script analysis following prefrontal lobe lesions. *Ann. NY Acad. Sci.* **769,** 277–288 (1995).
5. Spector, L. & Grafman, J. in *Handbook of Neuropsychology* (eds Boller, F. & Grafman, J.) 377–392 (Elsevier, Amsterdam, 1994).
6. Wharton, C. & Grafman, J. Reasoning and the human brain. *Trends Cogn. Sci.* **2,** 54–59 (1998).
7. Stuss, D. T. & Benson, D. F. *The Frontal Lobes* (Raven, New York, 1986).
8. Fuster, J. M. *The Prefrontal Cortex. Anatomy, Physiology, and Neuropsychology of the Frontal Lobe* (Raven, New York, 1989).
9. D'Esposito, M. *et al.* The neural basis of the central executive system of working memory. *Nature* **378,** 279–281 (1995).
10. Corbetta, M. Frontoparietal cortical networks for directing attention and the eye to visual locations: identical, independent, or overlapping neural systems? *Proc. Natl Acad. Sci. USA* **95,** 831–838 (1998).
11. Squire, L. R. *et al.* Activation of the hippocampus in normal humans: a functional anatomical study of memory. *Proc. Natl Acad. Sci. USA* **89,** 1837–1841 (1992).
12. Buckner, R. L. *et al.* Functional anatomical studies of explicit and implicit memory retrieval tasks. *J. Neurosci.* **15,** 12–29 (1995).
13. Shallice, T. *et al.* Brain regions associated with acquisition and retrieval of verbal episodic memory. *Nature* **368,** 633–635 (1994).
14. Grady, C. L. *et al.* Age-related reductions in human recognition memory due to impaired encoding. *Science* **269,** 218–221 (1995).
15. Tulving, E. *et al.* Neuroanatomical correlates of retrieval in episodic memory: auditory sentence recognition. *Proc. Natl Acad. Sci. USA* **91,** 2012–2015 (1994).
16. Tulving, E. *Elements of Episodic Memory* (Oxford Science, Oxford, 1983).
17. Galaburda, A. M., LeMay, M., Kemper, T. L. & Geschwind, N. Right-left asymmetrics in the brain. *Science* **199,** 852–856 (1978).
18. Furey, M. L. *et al.* Cholinergic stimulation alters performance and task-specific regional cerebral blood flow during working memory. *Proc. Natl Acad. Sci. USA* **94,** 6512–6516 (1997).
19. Goldman-Rakic, P. C. in *Handbook of Physiology, The Nervous System* (eds Plum, F. & Mountcastle, V.) 373–417 (American Physiological Society, Bethesda, MD, 1987).
20. Petrides, M. in *Handbook of Neuropsychology* (eds Boller, F. & Grafman, J.) 59–82 (Elsevier, Amsterdam, 1994).
21. Jonides, J. *et al.* Spatial working memory in humans as revealed by PET. *Nature* **363,** 623–625 (1993).
22. Courtney, S. M., Ungerleider, L. G., Keil, K. & Haxby, J. V. Transient and sustained activity in a distributed neural system for human working memory. *Nature* **386,** 608–611 (1997).
23. MacLeod, A. K., Buckner, R. L., Miezin, F. M., Petersen, S. E. & Raichle, M.. E. Right anterior prefrontal cortex activation during semantic monitoring and working memory. *NeuroImage* **7,** 41–48 (1998).
24. Grafton, S. T., Hazeltine, E. & Ivry, R. Functional mapping of sequence learning in normal humans. *J. Cogn. Neurosci.* **7,** 497–510 (1995).
25. Pallier, C., Dupoux, E. & Jeannin, X. EXPE: an expandable programing language for on-line psychological experiments. *Behav. Res. Methods Instrum. Comput.* **29,** 322–327 (1997).
26. Friston, K. J., Frith, C. D., Liddle, P. F. & Frackowiak, R. S. J. Comparing functional (PET) images: The assessment of significant change. *J. Cereb. Blood Flow Metab.* **11,** 690–699 (1991).
27. Talairach, J. & Tournoux, P. *Co-planar Stereotaxic Atlas of the Human Brain* (Thieme Medical, New York, 1988).
28. Duvernoy, H. *The Human Brain. Surface, Three Dimensional Sectional Anatomy and MRI.* (Springer, Wien, 1991).

Correspondence and requests for materials should be addressed to J.G. (e-mail: jgr@box-j.nih.gov).

Synaptic calcium transients in single spines indicate that NMDA receptors are not saturated

Zachary F. Mainen, Roberto Malinow & Karel Svoboda

Cold Spring Harbor Laboratory, 1 Bungtown Road, Cold Spring Harbor, New York 11724, USA

At excitatory synapses in the central nervous system, the number of glutamate molecules released from a vesicle is much larger than the number of postsynaptic receptors. But does release of a single vesicle normally saturate these receptors? Answering this question is critical to understanding how the amplitude and variability of synaptic transmission are set and regulated. Here we describe the use of two-photon microscopy[1] to image transient increases in Ca^{2+} concentration mediated by NMDA (*N*-methyl-D-aspartate) receptors in single dendritic spines of CA1 pyramidal neurons in hippocampal slices. To test for NMDA-receptor saturation, we compared responses to stimulation with single and double pulses. We find that a single release event does not saturate spine NMDA receptors; a second release occurring 10 ms later produces ~80% more NMDA-receptor activation. The amplitude of spine NMDA-receptor-mediated [Ca^{2+}] transients (and the synaptic plasticity which depends on this) may thus be sensitive to the number of quanta released by a burst of action potentials and to changes in the concentration profile of glutamate in the synaptic cleft.

The issue of receptor saturation has been controversial, partly owing to complexities in the interpretation of indirect experiments[2]. A direct test for saturation is to examine the interaction between two synaptic currents occurring in rapid sequence[3,4]. Receptor saturation during the first event will block the response to a second event that occurs before transmitter has had a chance to unbind from the receptors. Glutamate unbinding from NMDA receptors occurs slowly ($\tau > 100$ ms)[5,6]. Although it is conceptually simple, this experiment is complicated by the probabilistic nature of transmitter release. Because only a fraction of stimulated synapses release transmitter, the first and second responses might not occur at the same synapses, as is required for the interaction test. A reliable way to detect failure and release of transmitter at a single synapse is therefore required.

We used two-photon-laser scanning microscopy (2PLSM)[1] to monitor synaptic activation by measuring [Ca^{2+}] transients in postsynaptic spines[7]. Dendritic spines on CA1 pyramidal cells have a single postsynaptic density[8] associated with a single apposing presynaptic active zone[9]. Ca^{2+} entering spines through NMDA-receptor (NMDA-R) channels is therefore a direct reflection of NMDA-R activation at single synapses. We filled neurons in brain slices by whole-cell recording with a high-affinity Ca^{2+} indicator and activated synapses by extracellular stimulation using a glass pipette placed close to an apical dendritic branch[10]. Synaptic [Ca^{2+}] transients were imaged using either frame (16 Hz; Fig. 1) or line-scan (500 Hz; Fig. 2) mode. Frame mode allowed us to discriminate between anatomically distinct Ca^{2+} sources and thereby to isolate [Ca^{2+}] signals arising from single spines (Fig. A in Supplementary Information).

To isolate NMDA-R-mediated Ca^{2+} influx, neurons were voltage-clamped at positive potentials (above synaptic reversal potential; Fig. 2c) to allow opening of NMDA receptors, inactivate voltage-sensitive Ca^{2+} channels (Fig. B in Supplementary Information), and minimize the effects of possible synaptic voltage escape. Under these conditions, fluorescence transients were unaffected by the selective